

## Article

# Spatial and Temporal Change in Meteorological Drought in Gansu Province from 1969 to 2018 Based on REOF

Yuxuan Wang<sup>1</sup>, Fan Deng<sup>1,\*</sup>, Yongxiang Cai<sup>1,2</sup> and Yi Zhao<sup>3</sup>

<sup>1</sup> School of Geosciences, Yangtze University, Wuhan 430100, China; yangtze\_wyx@163.com (Y.W.); yxcai@yangtzeu.edu.cn (Y.C.)

<sup>2</sup> Key Laboratory of Engineering Geophysical Prospecting and Detection of Chinese Geophysical Society, Wuhan 430100, China

<sup>3</sup> Exploration Department of Huabei Oil Field Company, PetroChina, Renqiu 062552, China; wty\_zy@petrochina.com.cn

\* Correspondence: dengfan@yangtzeu.edu.cn

**Abstract:** Meteorological drought is one of the most serious natural disasters, and its impact in arid and semi-arid areas is significant. In order to explore the temporal and spatial distribution of meteorological disasters in Gansu Province, we first calculated the standardized precipitation evapotranspiration index (SPEI) based on the monthly meteorological data from 1969 to 2018 and extracted the drought events through the theory of runs. Then, REOF rotation orthogonal decomposition was performed to divide the study area into five climatic subregions. With each subregion as the basic unit, the variation characteristics and evolution trends of drought events at different time scales were compared based on the B-G segmentation algorithm (BG-algorithm). Finally, a correlation analysis was conducted to explore the driving factors of drought events in each subregion. The main conclusions are as follows: (1) The cumulative duration of drought in the study area showed a slight increase trend (0.475 day/decade) and a 19-year main cycle. The drought intensity showed a trend of first easing and then intensifying, especially after 2000; the drought intensified significantly and showed a spatial trend of decreasing drought in the northwest and worsening drought in the southeast. (2) The cumulative contribution rate of the first five modes of REOF decomposition was 64.46%, and the study was divided into five arid subregions: the Hexi region, middle Hedong region, eastern Hedong region, Wushaoling region and western Hedong region. (3) The meteorological drought in the Hexi region has eased significantly since 1988. In the eastern, central and western parts of the Yellow River, drought intensification was observed to have occurred in different degrees (0.12/decade, 0.129/decade, and 0.072/decade). The meteorological drought in the Wuelyaling region has alleviated significantly with a watershed region formed between drought alleviation and drought intensification. (4) Seasonally, the eastern Hedong region showed a significant trend of drought in spring, but the opposite in autumn. The trend of climate drying was obvious in the spring and summer, rather than in autumn and winter. The spring drought trend is the most obvious in the middle of the Hedong region. (5) The meteorological drought in the study area was affected by local climatic factors and circulation factors, but there were significant differences in the responses of different arid subregions to these factors.

**Keywords:** Gansu; SPEI; REOF; drought events; temporal and spatial variation



**Citation:** Wang, Y.; Deng, F.; Cai, Y.; Zhao, Y. Spatial and Temporal Change in Meteorological Drought in Gansu Province from 1969 to 2018 Based on REOF. *Sustainability* **2023**, *15*, 9014. <https://doi.org/10.3390/su15119014>

Academic Editors: Stefano Morelli, Veronica Pazzi and Mirko Francioni

Received: 18 April 2023

Revised: 24 May 2023

Accepted: 26 May 2023

Published: 2 June 2023



**Copyright:** © 2023 by the authors. Licensee MDPI, Basel, Switzerland. This article is an open access article distributed under the terms and conditions of the Creative Commons Attribution (CC BY) license (<https://creativecommons.org/licenses/by/4.0/>).

## 1. Introduction

Meteorological drought, as a kind of extreme weather condition, has been widely studied and is considered one of the most devastating meteorological disasters [1–5]. Since global warming has been exacerbated in recent years, the intensity, duration and frequency of droughts show an upward trend in some regions, which has negative effects on the ecological environment, agricultural production and social activities [6]. The monsoon climate and continental climate, which have a considerable impact on China, lead to

significant interannual changes in precipitation and the frequent occurrence of drought and flooding. Since 1990, an extreme drought event has happened at least once every two years in China on average, causing substantial economic losses [7]. Therefore, it is of practical significance to quantify the spatiotemporal characteristics of changes experienced under drought events. Currently, there have been various indexes proposed to characterize meteorologic drought [8–10], including the Palmer drought index (PDSI), standardized precipitation index (SPI), surface moisture index and meteorological drought index (CI). Although these indexes are effective at solving problems such as drought monitoring and prediction, they are still not comprehensive. PDSI applies to characterizing the severity of drought in a region, which is not only based on the balance of water supply and demand but also on various climate-related factors such as precipitation, humidity and evaporation. However, since the severity of drought is determined by subjective factors, the judgement of extreme drought is poor in timeliness. Reflecting the state of drought at different time scales and in various regions, SPI better represents the intensity and duration of drought. However, the main problem with it is that it only considers precipitation-related data while ignoring various climate-related factors that play a major role in the occurrence of drought, such as temperature and evapotranspiration [11]. To address this problem, Vicente Serrano [12] proposed the standardized precipitation evapotranspiration index (SPEI) in 2010. Based on precipitation and evapotranspiration, this index incorporates not only the advantage of the PDSI (Palmer drought severity index) in considering the sensitivity of evapotranspiration to temperature, but also that of the SPI (standardized precipitation index) in facilitating multi-scale and multi-spatial comparison. According to the existing studies, this index is suitable for exploring the spatiotemporal characteristics of drought event changes in the context of global warming and is applicable to identifying the occurrence of extreme drought events in arid and semi-arid regions more accurately. Compared to other drought indexes, it is more suited to the study of meteorological drought in Western China [13–17].

Up to now, the SPEI has been commonly used both at home and abroad to conduct studies. From 1901 to 2015, the area and intensity of drought in China showed an overall upward trend [18]. In most parts of Northeast China, there has been a significant trend of aridification over the past 50 years [19]. Throughout the last 55 years, the occurrence of extreme drought events showed a significant trend of seasonal variations in the southwest [20]. In the studies conducted by Lu Jiayu et al., it was found that the trend of aridification in Yunnan had reached a significant extent in the past 55 years [21]. According to the studies carried out by Zhang Yuanyuan et al. [22], the overall SPEI in Central Asia shows a downward trend, despite the significant seasonal differences that persist. According to the studies of Qi Leqin et al. [23], there is a significant spatial difference shown by the occurrence of meteorological drought in Northwest China, and aridification exhibits a significant trend of exacerbation in central China and Southern Xinjiang, although the extent of aridification is relatively low on the plateau and in the east. For the drought events occurring in Northwest China, it remains necessary to perform further subdivisions and accurate assessments.

Located in the northwest of China, Gansu Province intersects with three major deserts, namely Badain Jilin, Tengger and Kumtag. Due to low precipitation and high evaporation, the local ecological system is more susceptible to drought events. In the context of global warming, it is difficult to restore the local ecological environment because of drought. In the meantime, this region is also most prone to the occurrence of drought in China, with the annual economic losses caused by drought being far more severe than in other parts of China [24]. If drought worsens, it affects the distribution, yield and growth of crops, which leads to vegetation degradation, thus accelerating regional desertification. Therefore, this study adopted the theory of runs to extract drought events, which is based on the meteorological data collected from Gansu Province in the past 50 years. Rotated empirical orthogonal function (REOF) decomposition was performed to divide the study area into multiple subregions, for exploring the spatiotemporal changes of droughts occurring in

Gansu Province. This was expected to provide a theoretical basis for the optimal allocation and scientific evaluation of water resources, which is essential for the early warning of drought as well as the formulation of disaster prevention and mitigation policies in the study area.

## 2. Materials and Methods

### 2.1. Overview of the Study Region

As a typical area of transition between the temperate monsoon climate and the continental climate (Figure 1), Gansu is located at the intersection of three natural regions in China: the eastern monsoon region, the northwest arid region and the Qinghai–Tibet alpine region. Meanwhile, it represents the junction of three major plateaus: the Qinghai–Tibet Plateau, the Loess Plateau and the Inner Mongolian Plateau (Figure 1). The study area is characterized by the complexity of physical and geographical conditions and biodiversity, with a wide variety of vegetation distributed in a significant latitudinal and vertical zonal form from the south to the north. In this region, the level of annual precipitation is relatively low, the average of which is less than 400 mm. In general, it decreases from the southeast to the northwest.

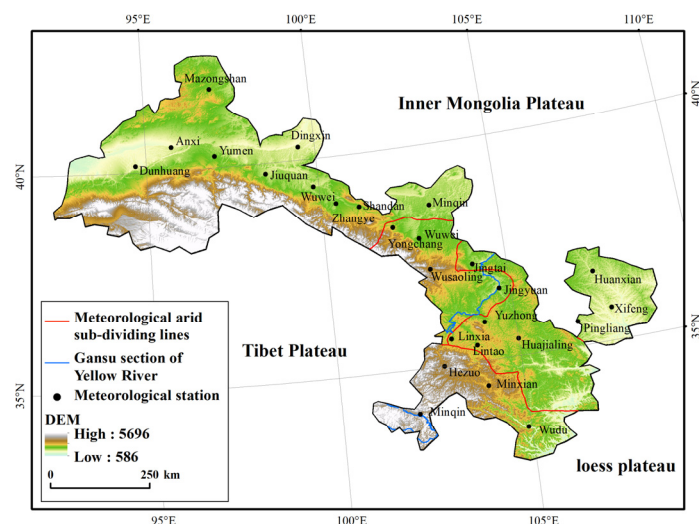


**Figure 1.** Overview of the study area.

### 2.2. Data Source

The monthly data collected by 32 meteorological stations in Gansu from 1969 to 2019 were sourced from the China Surface Climate Monthly Data Set of Chinese meteorological data website (<http://data.cma.cn/>, accessed on 25 May 2023). This dataset is a monthly set obtained from the compilation and statistics of national surface daily data from various provinces throughout China, in accordance with the relevant provisions of the “Statistical Methods for National Surface Climate Data (1961–1990)” and the “Ground Meteorological Observation Specifications”, and has passed the extreme value test and time consistency test of data. With rigorous quality control applied to the data, the univariate linear regression method was used to recover the missing monthly data. The climatic factors concerned in the study included precipitation (mm), average temperature (°C), average minimum, maximum temperature (°C), average wind speed (m/s), relative humidity (%) and sunshine hours (h). All atmospheric circulation factors were expressed in exponential form. As for the monthly ENSO (El Niño–Southern Oscillation), NAO (North Atlantic Oscillation), AO (Arctic Oscillation), PDO (Pacific Interdecadal Oscillation) and NP (North Pacific Tele Correlation Index) circulation factor data, they were sourced from the Climate Prediction Center of the National Weather Service of the United States (<https://www.cpc.ncep.noaa.gov/products/precip/CWlink/MJO/climwx.shtml> accessed on 25 May 2023). Then, the data of 5 atmospheric circulation factors for each season were obtained through mean

value processing. DEM data were the ASTER GDEM 90 M resolution digital elevation data collected from a geospatial data cloud. After the study area was divided, a DEM diagram of the study area was generated after the projection and mask for the DEM data.

### 2.3. Study Method

#### 2.3.1. Standardized Precipitation Evapotranspiration Index (SPEI)

- (1) Calculate evapotranspiration through the Penman–Monteith equation.

By taking into account the effect of surface evapotranspiration changes on drought introduced, the SPEI improved the sensitivity of this method to the aridification caused by the rapid temperature rise, thereby making it suitable for the geographical conditions in the study area [25]. The calculation of  $ET_0$  was performed by using the Penman–Monteith equation recommended by FAO 56. The details are shown in Reference [26].

- (2) Calculate the difference between monthly precipitation and potential evapotranspiration through the following equation:

$$D_i = P_i - (ET_0)_i \quad (1)$$

where  $P_i$  represents the monthly precipitation and  $(ET_0)_i$  denotes the monthly potential evapotranspiration.

- (3) Apply the log-logic distribution with three parameters to fit  $D_i$  and calculate the cumulative function,

$$f(x) = \frac{\beta}{\alpha} \left( \frac{x - \gamma}{\alpha} \right)^{\beta-1} \left[ 1 + \left( \frac{x - \gamma}{\alpha} \right)^{\beta} \right]^{-2} \quad (2)$$

$$F(x) = \int_0^x f(t) dt = \left[ 1 + \left( \frac{\alpha}{x - \gamma} \right)^{\beta} \right]^{-1} \quad (3)$$

where  $f(x)$  represents a probability density function,  $F(x)$  denotes a probability distribution function and  $\alpha$ ,  $\beta$  and  $\gamma$  refer to three parameters obtained through fitting based on the linear moment method (L-moment).

$$\alpha = \frac{(\omega_0 - 2\omega_1)\beta}{\Gamma(1 + 1/\beta)\Gamma(1 - 1/\beta)} \quad (4)$$

$$\beta = \frac{2\omega_1 - \omega_0}{6\omega_1 - \omega_0 - 6\omega_2} \quad (5)$$

$$\gamma = \omega_0 - \alpha \Gamma\left(1 + \frac{1}{\beta}\right) \Gamma\left(1 - \frac{1}{\beta}\right) \quad (6)$$

- (4) Normalize for the sequence to obtain the corresponding SPEI value:

$$SPEI = \omega - \frac{c_0 + c_1\omega + c_2\omega^2}{1 + d_1\omega + d_2\omega^2 + d_3\omega^3}$$

Probabilistic weighted moment  $\omega = \sqrt{-2\ln p}$ . When  $p \leq 0.5$ ,  $p = F(x)$ ; when  $p > 0.5$ ,  $p = 1 - F(x)$ .

The drought classification by the SPEI is detailed in Table 1 [12].

**Table 1.** Criteria of monthly SPEI drought classification.

Grade	No Drought	Mild Drought	Moderate Drought	Severe Drought	Extreme Drought
SPEI	$SPEI \geq -0.5$	$-1 \leq SPEI < -0.5$	$-1.5 \leq SPEI < -1$	$-2 \leq SPEI < -1.5$	$SPEI \leq -2$

### 2.3.2. Drought Identification

As a means to analyze the time series of variables, the theory of runs has been widely adopted in recent years to deal with the extraction and discrimination of drought events.

Compared to the traditional method that is applicable only for comparing drought indexes, it achieves a higher accuracy in identifying regional drought and improves the overall understanding of drought events. A run refers to the part that is lower or higher than a truncation threshold in all the values of the time series. The part higher than the truncation threshold is a positive run, while the part lower than the truncation threshold is a negative run [21]. The SPEI sequence values were calculated to identify drought based on the theory of runs. According to the criteria of drought classification (Table 1), only when the SPEI value falls below  $-0.5$  can drought happen. In this study, there are three thresholds set for determining drought events:  $X_0 = 0.5$ ,  $X_1 = -0.5$ , and  $X_2 = -1.5$ . The rules for carrying this out are as follows (Figure 2):

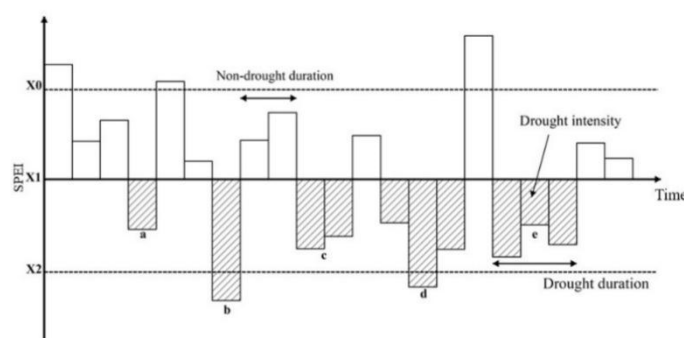


**Figure 2.** Drought recognition based on the theory of runs.

Three cutoff levels ( $X$  represents the SPEI value) were set according to the classification of drought severity using the SPEI (Table 1). When  $SPEI < X_1$ , this month is considered arid (a, b, c, d, e in Figure 2). If the drought lasts only one month and the corresponding SPEI falls below  $X_2$ , this month is considered a drought event (b in Figure 2); otherwise, it is considered a minor drought event (a in Figure 2) and thus ignored. For two adjacent drought events with an interval of 1 month, they are subordinate droughts if the interval is  $X_1 < SPEI < X_0$ . In this case, these two adjacent droughts are combined into one (c and d in Figure 2); otherwise, they are treated as two separate drought events (d and e in Figure 2) [27].

### 2.3.3. REOF Rotational Orthogonal Decomposition

EOF (empirical orthogonal function) [28] and REOF [29], as two different methods of decomposition analysis, were used to analyze the drought events extracted through the theory of runs for determining the spatiotemporal distribution characteristics of drought events occurring in Gansu. The EOF method was applied to decompose a field containing the spatial points that change over time. With its spatiotemporal characteristics separated and expanded to obtain the main eigenvectors, the variability structure of the entire climate variable field was maximized. However, there is a limitation on EOF; that is, the spatial distribution of eigenvectors is affected by the range of sampling and the size of samples. REOF decomposition is a method that concentrates variance contributions on a smaller region through variance maximum rotation transformation on the basis of EOF to reveal the pattern of spatial distributions. The results are not only reflective of the changes and distribution in different regions, but also applicable to dividing the arid subregions. The process of determining EOF and REOF is detailed in References [27,28].

### 2.3.4. Other Methods

The B-G segmentation algorithm was used to segment the factor time series for the factor change stage to be determined. Proposed by Bernarda Galvan et al. [30], the B-G

segmentation algorithm is a method suitable for detecting the abrupt change in non-linear and non-stationary time series. Unlike the traditional methods of abrupt change detection such as the M-K abrupt change detection method and the Pettitt method, this algorithm divides a non-stationary sequence into multiple stationary subsequences with different mean values based on the  $t$ -test, with each sub-sequence being used to characterize different physical backgrounds and the scale of each mean segment being obtained to show variability. The linear regression method was used to analyze the trend of changes in the factors. A significance test was conducted, with the confidence level  $\alpha$  being set to 0.01 and 0.05. A sliding  $t$ -test was performed to determine whether or not the trend of change in the factors was significant and to locate the abrupt change, with the confidence level  $\alpha$  being set to 0.01 and 0.05. The symbol \* indicates passing the confidence test of  $p < 0.05$ , and the symbol \*\* indicates passing the confidence test of  $p < 0.01$ . The Pettitt method was used to assist the test on abrupt changes, for further determining the year in which the abrupt change occurred. The periodic changes of drought events were analyzed by means of Morlet wavelet analysis. The inverse distance spatial interpolation method (IDW) was used to interpolate climatic factors and generate a grid map.

### 3. Results

#### 3.1. Spatiotemporal Change in Meteorological Drought in the Recent 50 Years in the Study Area

##### 3.1.1. Spatiotemporal Change in Drought Duration

Drought duration can be used to effectively reflect how long drought events last, which provides an important reference for the change in other drought events. Figure 3a shows the trend of changes and cumulative anomaly of annual drought duration in the study area. Over the past 50 years, the duration of drought in the study area increased slightly (0.475 day/decade), with a minimum value of 27 (days) and a maximum value of 167 (days). The cumulative anomaly curve showed a trend of rising, then falling sharply and, finally, rising unsteadily, with the extreme point appearing in 1989, which failed the significance test. It is indicated that in the past 50 years, the duration of drought in the study area was continuously extended at first, shortened in the late 1980s and gradually extended again from the middle of the 1990s to the present. Morlet wavelet analysis shows significant periodic changes (Figure 4).

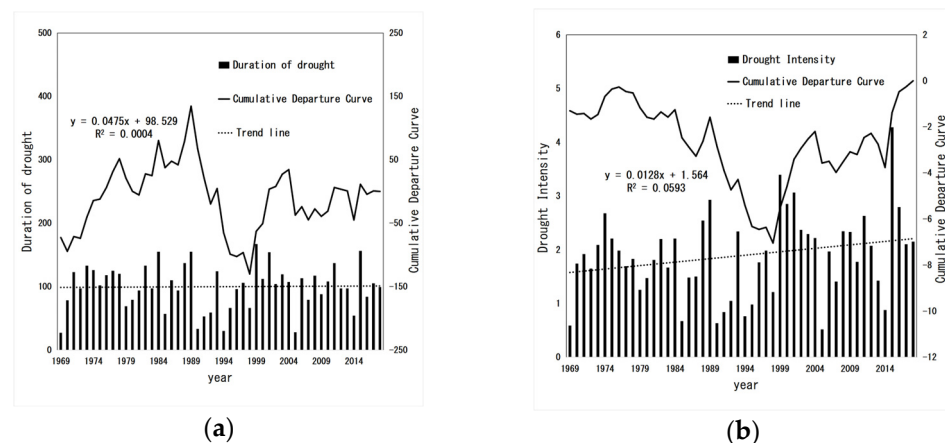


**Figure 3.** Trends and cumulative anomaly curve of drought duration (a) and drought intensity (b).

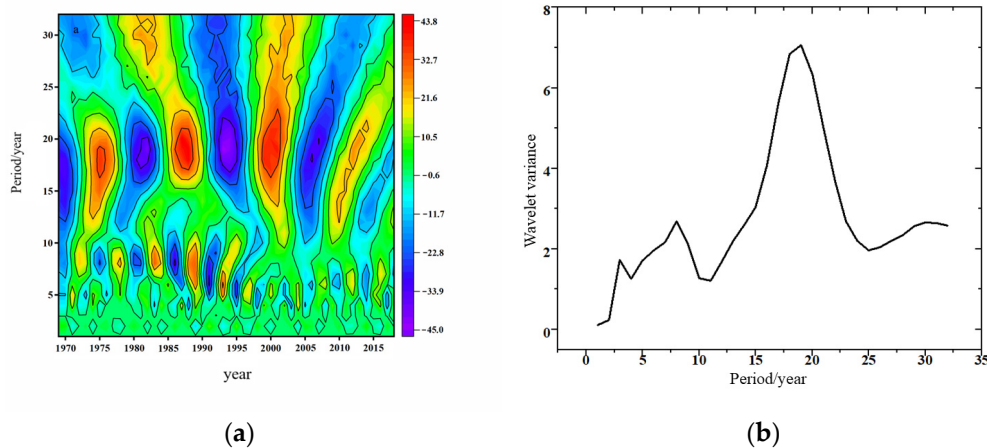


**Figure 4.** Wavelet variance (a), in semi-humid region (b) of drought duration.

The primary period of 19 years spans the entire time series, forming three high- and low-value centers, and the period is significant. Since 2007, the oscillation has been reduced and the fluctuations of factors has tended to stabilize. The oscillation at the sub-period of 8 years was found to be significant before 1990, and then it became insignificant. Figure 5a,b shows the spatial distribution of the multi-year average drought duration and the trend rate of annual drought duration change in Gansu. In general, the study area shows a distribution pattern of a long duration in the northwest and a short duration in the southeast. Except for Linxia and Gaolan, the average duration of annual drought is shorter than 3 months in the east of the Yellow River. According to the spatial distribution diagram of the multi-year trend rate of drought duration, except for the Wushaoling and Jiuquan regions at the Western edge of the Hexi Corridor where a downward trend of drought duration was exhibited, the duration was gradually extended in the rest of the study area.

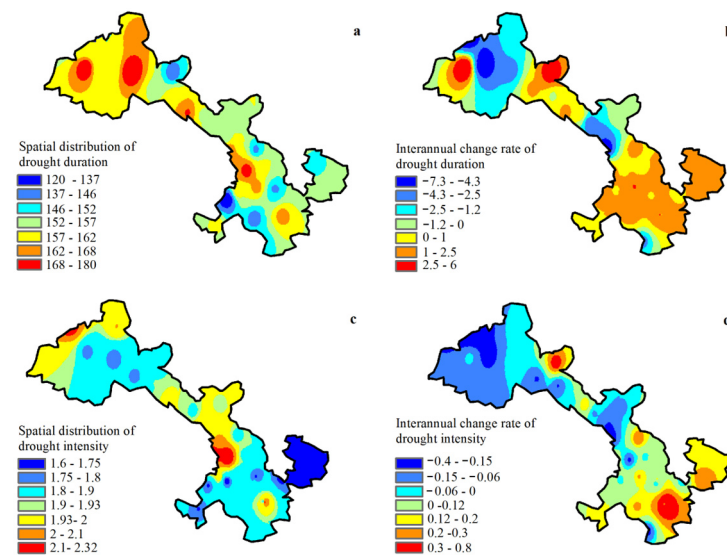


**Figure 5.** Spatial distribution of drought duration and drought intensity (a,c); interannual change rate of drought duration and drought intensity (b,d).

### 3.1.2. Spatiotemporal Change in Drought Intensity

Effectively reflecting the intensity of drought events, drought intensity is an important indicator used to measure the severity of drought. Figure 3b shows the trend of change in drought intensity in the study area over the past 50 years. Overall, drought intensity showed an upward trend (0.12/decade) ( $p > 0.05$ ), which failed the significance test because the trend of aggravation was relatively insignificant. It can be seen from the cumulative

anomaly curve that the intensity of drought reached a minimum in 2000, which passed the significance test, indicating that the meteorological drought in the study area was aggravated significantly after 2000. The trend of aridification was more significant. Figure 5c,d shows the spatial distribution of multi-year average drought intensity and the annual trend rate of drought intensity change in Gansu. Overall, the intensity was higher in the central part and lower in the southeast and the northwest. Except for in a few stations, there was a trend of alleviation shown in the northwest and a trend of aggravation shown in the southeast.

### 3.2. Spatiotemporal Changes in Meteorological Drought in Climate Subregions Based on REOF

#### 3.2.1. Division of Subregions

EOF and REOF decomposition were performed on the intensity of drought occurring in Gansu and its surrounding stations to further determine the spatial differentiation of drought events in this province. The analytical results were obtained, as shown in Table 2. According to the North test, the first five modes decomposed via EOF passed the significance test, and the cumulative contribution of the first five modes reached 73%. The first five principal components were rotated. Due to the relatively complex climatic factors affecting the study area and their low convergence rate, the cumulative variance contribution of the first five eigenvectors of REOF was merely 64.46% (Table 2), which contains the main information and laws of the spatial distribution of annual drought events in the study area. The eigenvector corresponding to the maximum absolute value of the annual time coefficient was treated as the spatial distribution pattern mode of the drought intensity in the year. Finally, the subregions of drought intensity in the study area were divided according to the REOF results. The calculation results of EOF and REOF are listed in Table 2.

**Table 2.** The first 5 feature vectors and contributions of EOF and REOF.

Serial Number	EOF		REOF	
	Rate of Contribution %	Accumulating Contribution Rate %	Rate of Contribution %	Accumulating Contribution Rate %
1	0.41	0.41	30.51	30.51
2	0.12	0.53	12.73	42.24
3	0.09	0.62	7.62	50.86
4	0.07	0.69	7.23	58.09
5	0.04	0.73	6.37	64.46

Figure 6 shows the spatial distribution of load values under the five spatial modes of REOF before drought intensity, where RLV1 represents the rotating load vector field of the first mode, and so on. Table 2 details the time coefficient characteristics and drought spatial differentiation models under the first five spatial modes of REOF. RLV1 (Figure 6a) was found to be the most common mode of drought intensity distribution over the last 50 years. The central load was located in the Hexi region (+0.987), and the isoline showed the highest density, indicating that the intensity of drought was consistent across the region for years. The variability of drought intensity in the Hexi region reached a high level, while it was low in the southeast. It was uniformly dry in the whole region for 13 years, most of which were concentrated from 2008 to 2019, and uniformly wet in the whole region for 8 years, most of which were concentrated from 1988 to 2005. RLV2 (Figure 6b) presents a high distribution pattern in the southeast and a low pattern in the northwest. Except for in the Beishan region, the load is invariably positive. The central load is located in the central part of the central Hedong region (+0.778), and the isolines are dense in the east and sparse in the west, indicating that there are some years in which the drought intensity distribution shows a north–south reverse mode characteristic bounded by the “zero line”, and the variability is more significant in the southeast, especially in the central part of the central Hedong region. It was wetter in the north and drier in the south for 9 years, most of

which were concentrated between 1980 and 2000, and drier in the north and wetter in the south for 8 years, all of which were before 1985. RLV3 (Figure 6c) shows a decreasing trend from the east to the west along the longitude lines, with negative values distributed in Zhangye and Yongchang located in the middle east of the Hexi Corridor. A positive central load was located in the eastern part of Hedong (+0.899), while the isoline was thick in the east but thin in the west, indicating that drought intensity was bounded by the “zero line” in some years. This shows a pattern of reverse distribution between the central, eastern and western parts. The variability is more significant in the eastern part of Hedong. There was one year in which it was arid in the central part and wetter in the eastern and western parts (1995), and three years in which it was humid in the central part and arid in the eastern and western parts (1981, 1990, and 1994). RLV4 (Figure 6d) showed a decreasing trend from the east to the west in the Wushaoling region as the central part, and the negative value was concentrated in Wudu, Tianshui and other parts in the south of the study area. The positive central load was located in the Wushaoling region (+0.74), which was classed as a Wushaoling type. Drought intensity exhibits a pattern of north–south reverse distribution with a boundary of 35° N in a few years, and the variability in the Wushaoling region reaches a higher level than that in other regions. The negative value of RLV5 (Figure 6e) was mainly distributed in the eastern and western parts of the Yellow River, while the positive central load was located in the western part of the Yellow River (+0.723). The isoline was dense in the south but sparse in the north, indicating that the drought intensity showed a pattern of middle-east–west reverse distribution for a few years, and that the variability was more significant in the south than in the north.

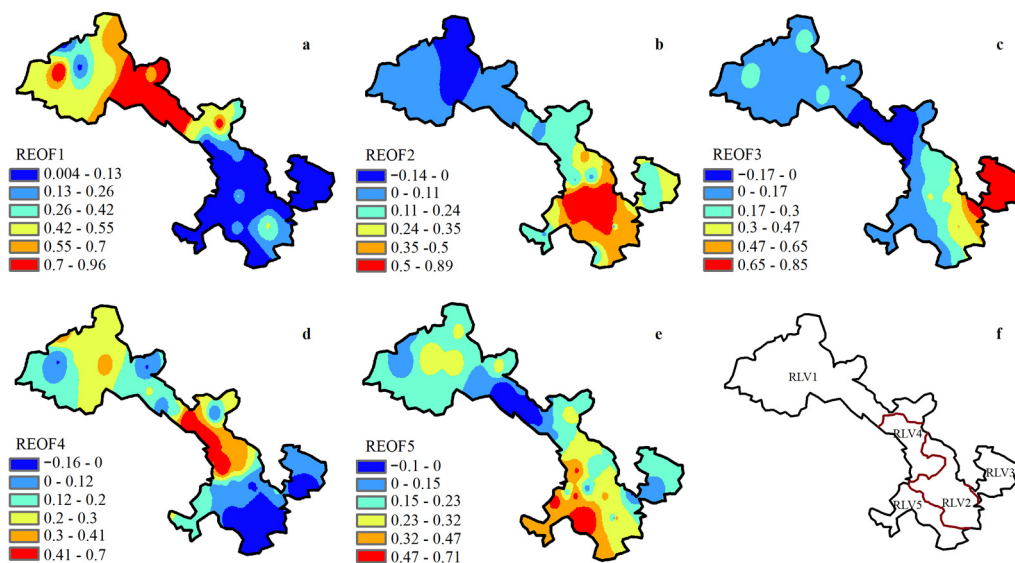


**Figure 6.** REOF Mode 1 (a), REOF Mode 2 (b), REOF Mode 3 (c), REOF Mode 4 (d), REOF Mode 5 (e), and REOF subregion (f).

The study area was divided into five arid subregions using the rotation component matrix obtained from the REOF analysis, with some repetitive parts removed from the spatial distribution of the load capacity. By taking the regions with significant absolute load capacity values as the center, Gansu Province was divided into five arid subregions (Figure 6f), namely Hexi (RLV1), central Hedong (RLV2), eastern Hedong (RLV3), Wushaoling (RLV4) and western Hedong (RLV5).

### 3.2.2. Interannual Change Characteristics of Drought Intensity in the Climatic Subregions

The univariate linear trend was used to determine the trend of changes in the time series. The significance of the changing trend was tested by means of a sliding T-test. The Pettitt abrupt change test and sliding *t*-test were performed to determine the year of the abrupt change. The B-G segmentation algorithm was applied to segment the time series by

stages, with S1 (stage 1) representing the average value of the drought intensity in the first stage, and so on (Figure 7).

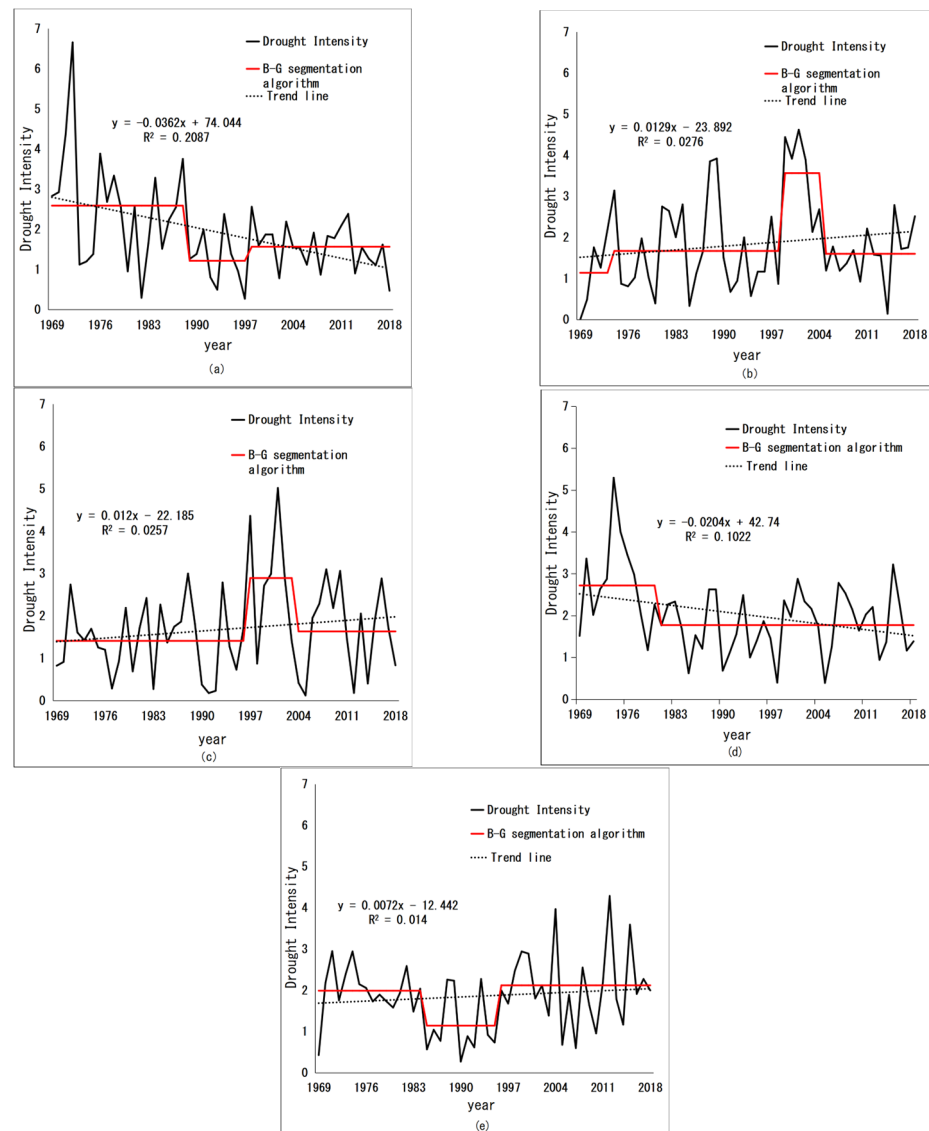


**Figure 7.** Interannual variation and segmentation stage of drought intensity in Hexi region (a), central Hedong central region (b), eastern Hedong region (c), Wushaoling region (d) and western Hedong region (e).

The drought intensity in the Hexi region showed a significant downward trend at  $-0.362/\text{decade}$  ( $|T| = 3.63 > 2.738$ ,  $\alpha = 0.01$ ), an abrupt decrease in 1988 ( $|T| = 3.74 > 2.738$ ,  $\alpha = 0.01$ ) and then a sharp decline at  $-0.601/\text{decade}$  ( $p > 0.05$ ). B-G segmentation was performed to determine three stages: 1969–1988, 1989–1997 and 1998–2019. According to the comparison drawn between the mean values of each stage, the intensity of S2 was 52.9% higher than that of S1, and that of S3 was higher compared to that of S2, indicating that the region experienced a significant change from arid to humid in the past 50 years. After 1990, it tended to be humid (Figure 7a).

The drought intensity in the central part of Hedong showed an upward trend at  $0.129/\text{decade}$  ( $p > 0.05$ ), before an increase in 1988, which failed the significance test. B-G segmentation was performed to determine four stages: 1969–1974, 1975–1998, 1999–2004 and 2005–2019. According to the comparison drawn between the mean values of each stage, that of S2 was 46.4% higher than that of S1, that of S3 was 1.13 times that of S2, and that of

S4 was 55.02% lower than that of S3. This indicates the insignificant trend of aridification in this region over the past 50 years. However, the intensity has been in decline year on year, showing a trend of humidification (Figure 7b).

The drought intensity in the eastern Hedong region showed an upward trend at 0.12/decade ( $p > 0.05$ ), before an abrupt increase in 1996 ( $|T| = 2.04 > 2.037$ ,  $\alpha = 0.05$ ). B-G segmentation was performed to obtain three stages: 1969–1996, 1997–2003 and 2004–2019. According to the comparison drawn between the mean values of each stage, that of S2 was 1.04 times that of S1, and that of S3 was 43.5% higher than that of S2, which indicates an insignificant trend of aridification in this region over the past 50 years. However, the intensity of drought has decreased unsteadily since 2002, showing an insignificant trend of humidification (Figure 7c).

The drought intensity in the Wushaoling region showed a significant downward trend at  $-0.19$ /decade ( $|T| = 2.11 > 1.67$ ,  $\alpha = 0.05$ ), an abrupt decrease in 1975 ( $|T| = 4.35 > 2.738$ ,  $\alpha = 0.01$ ) and an unsteady decline. There were two time points of abrupt change found via B-G segmentation, but the year 1969 ( $L0 = 0.99 > 0.95$ ) was excluded due to its impracticality. There were two time periods determined by segmentation: 1969–1980 and 1981–2019. That of S2 was 34.7% lower than that of S1, indicating a significant trend of humidification occurring in the region over the past 50 years, with a clear watershed formed (Figure 7d).

The drought intensity in the west of Hedong showed a slight increase at 0.072/decade ( $p > 0.05$ ), an abrupt increase in 1997 ( $|T| = 2.06 > 2.037$ ,  $\alpha = 0.05$ ) and a slight increase in the following years. B-G segmentation was performed to determine three stages: 1969–1984, 1985–1995 and 1996–2019. According to the comparison of the mean value between different stages, that of S2 was lower than that of S1 and that of S3 was higher than that of S2, which indicates a trend of slight aridification in the region over the past 50 years. However, it tended to be humid between 1985–1995, showing the process of gradual aridification from 1996 to the present (Figure 7e).

### 3.2.3. Seasonal Change Characteristics of Drought Intensity in the Climatic Subregions

The seasonal drought intensity of each drought subregion was calculated using the monthly data of drought intensity to explore the trend of changes and the time points of abrupt change in the past 50 years. The results are listed in Table 3.

**Table 3.** Seasonal variation characteristics of drought intensity in each climatic subregion.

		Spring	Summer	Autumn	Winter
Hexi region	Trend of change	Deepening drought	Decreasing drought	Deepening drought	Deepening drought
	Significance	Insignificant ( $p > 0.05$ )	Significant ( $p < 0.01$ )	Insignificant ( $p > 0.05$ )	Insignificant ( $p > 0.05$ )
	Mutation year	None	2014	None	None
Hedong central region	Trend of change	Deepening drought	Deepening drought	Deepening drought	Deepening drought
	Significance	Significant ( $p < 0.01$ )	Insignificant ( $p > 0.05$ )	Insignificant ( $p > 0.05$ )	Insignificant ( $p > 0.05$ )
	Mutation year	1993	None	1981	None
Hedong eastern region	Trend of change	Deepening drought	Decreasing drought	Decreasing drought	Decreasing drought
	Significance	Significant ( $p < 0.01$ )	Insignificant ( $p > 0.05$ )	Significant ( $p < 0.01$ )	Insignificant ( $p > 0.05$ )
	Mutation year	1997	None	2002	None

Table 3. Cont.

		Spring	Summer	Autumn	Winter
Wushaoling region	Trend of change	Deepening drought	Decreasing drought	Decreasing drought	Decreasing drought
	Significance	Insignificant ( $p > 0.05$ )	Significant ( $p < 0.01$ )	Insignificant ( $p > 0.05$ )	Significant ( $p < 0.01$ )
	Mutation year	None	1990	None	1979
Hedong western Region	Trend of change	Deepening drought	Deepening drought	Decreasing drought	Decreasing drought
	Significance	Significant ( $p < 0.01$ )	Significant ( $p < 0.05$ )	Significant ( $p < 0.05$ )	Insignificant ( $p > 0.05$ )
	Mutation year	2002	2000	2002	None

The drought intensity in the Hexi region only showed a trend of significant moderation in summer, and there was an abrupt decrease in 2014, which made the trend of moderation more significant. In addition, it showed a trend of slight aridification in other seasons, with the trend of moderation starting in the spring of 2011, the autumn of 2002 and the winter of 2014. However, there was no abrupt change observed.

The changes in meteorological drought in central Hedong were significantly consistent, showing the trend of aridification in all seasons. The rate of decrease in drought intensity was found in the following order: spring ( $-0.079/\text{decade}^{**}$ ) > summer ( $-0.064/\text{decade}$ ) > autumn ( $-0.052/\text{decade}$ ) > winter ( $-0.023/\text{decade}$ ). The abrupt change to drought occurred in the spring and autumn of 1993 and 1981, and the shift from humid to arid occurred in 2000 and 1998, but not to a significant extent.

In the eastern Hedong region, there was a trend of significant aridification shown only in spring, and there was an abrupt change in drought in 1997, showing a trend of exacerbation. The trend of aridification was the most significant in autumn and it changed abruptly in 2002. In comparison, drought intensity insignificantly reduced in the other two seasons.

The seasonal changes in the Wushaoling region were consistent, with a trend of moderation shown by drought at varying degrees. The rate at which drought intensity increased was in the following order: winter ( $0.128/\text{decade}^{**}$ ) > summer ( $0.078/\text{decade}^{**}$ ) > spring ( $0.03/\text{decade}$ ) > autumn ( $0.021/\text{decade}$ ). Abrupt changes occurred in the winter and summer of 1979 and 1990, while the shift to humid was insignificant in the other two seasons.

The seasonal differences in the western Hedong region were significant, showing a trend of aridification in the spring and summer, with the order spring ( $-0.058/\text{decade}^{**}$ ) > summer ( $-0.056/\text{decade}^*$ ). The abrupt change in drought occurred in these two seasons of 2002 and 2000. In the autumn, drought showed a trend of significant moderation ( $0.07/\text{decade}^*$ ) and abrupt change in 2002. Then, the trend of moderation became more significant, before becoming insignificant in the winter.

### 3.3. Driving Factor Analysis

According to existing studies, climate change is a major contributor to the occurrence of drought [31,32]. Drought occurs due to the combined effect of local climatic factors and circulation factors rather than a single factor. Three local climatic factors, including temperature, precipitation and sunshine hours, were used in this paper to analyze the correlation with drought intensity in each subregion, for the driving factors of drought intensity to be determined. Furthermore, five circulation factors were introduced to explore the influencing factors of meteorological drought in different seasons across the study area. As can be seen from Table 4, there was a significant variation in the response of drought intensity to the climatic factors in these climatic subregions. From a regional

perspective, the response to the temperature reached a significant extent in the Hexi and western Hedong regions, which passed the significance test of  $\alpha = 0.01$  and  $\alpha = 0.05$ , respectively. They exhibited a significant positive correlation, which means meteorological drought aggravates a temperature rise. In central Hedong and eastern Hedong, there was a significant response to precipitation, which passed the significance test of  $\alpha = 0.05$  and  $\alpha = 0.01$ . Meteorological drought showed a trend of aggravation when precipitation decreased. In the Wushaoling region, there was a significant response to sunshine hours, which passed the significance test of  $\alpha = 0.05$ . Meteorological drought showed a trend of aggravation when the number of sunshine hours increased. From the perspective of climatic factors, there was not only a positive correlation observed between temperature and drought intensity, but also a negative correlation found between precipitation and drought intensity. The correlation between sunshine hours and drought intensity showed variations by region. Sunshine hours exhibited an insignificant negative correlation with the Hexi and central Hedong regions but a positive correlation with other regions.

**Table 4.** The correlation coefficient between drought intensity and climate-related factors.

	Temperature	Precipitation	Sunshine Duration
Hexi region	0.439 **	−0.095	−0.104
Hedong central region	0.205	−0.321 *	−0.150
Hedong eastern region	0.260	−0.5617 **	0.024
Wushaoling region	0.076	−0.027	0.303 *
Hedong western Region	0.321 *	−0.131	0.048

Note: \* indicates passing the confidence test of  $p < 0.05$ , and \*\* indicates passing the confidence test of  $p < 0.01$ .

According to the Pearson correlation analysis (Table 5), there was only a significant positive correlation between drought intensity and NAO (North Atlantic Oscillation) across the study area in summer, with a correlation coefficient of 0.35 ( $p < 0.05$ ). In addition, there was a negative correlation observed in autumn and winter ( $p > 0.05$ ), and a weak positive correlation was found in spring, which indicates a significant effect of the NAO index on the study area during summer. Hence, the drought occurring in the study area showed a trend of aggravation in summer with the rise in the NAO index. Drought intensity and ENSO exhibited a significant positive correlation in spring and autumn ( $p < 0.01$ ,  $p < 0.05$ ), but a negative correlation in summer and winter ( $p > 0.05$ ), which indicates not only a close correlation between the occurrence of meteorological drought and ENSO events during spring and autumn in the study area, but also a significant effect of ENSO events on drought events in spring. Drought intensity and AO (Arctic Oscillation) showed a significant positive correlation in winter ( $p < 0.05$ ), but showed a positive correlation in summer and autumn ( $p > 0.05$ ). This indicates a close correlation between the occurrence of meteorological drought and AO events during winter in the study area, and the varying degrees of the effect of events on drought events during all seasons in the study area except summer. Drought intensity and PDO (Pacific Interdecadal Oscillation) showed a significant negative correlation in summer ( $p < 0.05$ ), indicating a trend of moderation shown by meteorological drought during summer in the study area with the increase in the POD event. Drought intensity and NPI (North Pacific Index) exhibited a weak positive correlation in spring and winter, but a weak negative correlation in summer and autumn, both of which failed the significance test. It is indicated that NPI events exerted a relatively weak effect on meteorological drought during the four seasons in the study area.

**Table 5.** Correlation coefficient between drought intensity and circulation.

Circulation Factor	Spring	Summer	Autumn	Winter
NAO	0.13	0.35 *	−0.03	−0.10
ENSO	0.47 **	−0.08	0.30 *	−0.16
AO	0.31	−0.06	0.27	0.41 *
PDO	0.07	−3.3 *	0.1	0.18
NP	0.16	−0.13	−0.04	0.25

Note: \* indicates passing the confidence test of  $p < 0.05$ , and \*\* indicates passing the confidence test of  $p < 0.01$ .

#### 4. Discussion

In the study, it is indicated that the SPEI is more appropriate for Gansu than other drought indexes are, and is effective at reflecting the state of drought in a specific way [33]. In addition, extracting drought events for the SPEI according to the theory of runs is conducive to quantitatively analyzing the extent of change in drought events. The spatial structure is clarified via REOF decomposition, which improves the accuracy in reflecting the changes in the spatial pattern of drought events over the past 50 years. In Gansu, a typical dry farming region, meteorological drought is a significant factor causing natural disasters, which affect agricultural production. When the overall temperature rises significantly in the northwest, moisture is the main factor affecting local wetness. As a major natural disaster that affects agricultural production and ecological preservation in the northwest, drought is exacerbated continuously with the increase in its frequency and intensity.

In recent years, the precipitation in the north of China has increased to an especially higher level than it has in previous years due to the combined effect of large-scale circulation adjustment and temperature rise, while extreme precipitation events have increased as well. As indicated by Yu Shuqiu, a significant climatic leap occurred in Northwest China in 1986. Subsequently, the annual precipitation and summer precipitation increased [34]. According to the study of Wang Chenghai et al., the annual precipitation of stations in the northwest exhibits an increasing trend, and the stations showing a decreasing trend are concentrated in the southeast monsoon region [35]. As revealed by Cao Yanchao et al. [36], the overall level of precipitation during summer in Gansu Hexi showed an increasing trend since 2010. These results may exert a moderating effect on meteorological drought in the western part of the study, which supports the argument that meteorological drought is moderated during summer in Hexi.

On the interannual scale, the drought occurring in the study area was aggravated after being moderated, significantly after 2000. The study area experienced noticeable spatial and temporal differences in climate change over nearly 50 years, which can be attributed to global warming. Since 2000, drought intensity in the southeast region of the study area has increased [37], while in the 1990s, the area bounded by Wushaoling has exhibited opposite precipitation trends with decreasing precipitation in the east and increasing precipitation in the west [38]. The primary reason for the dry and wet climate changes in the study area is the alteration of the climate system over time. The Wushaaling region demonstrates the boundary between the East Asian monsoon system and the westerly system, and the precipitation in these two areas has a significant correlation with the strength of the corresponding monsoons and westerlies [39]. The westerly climate has become humid since the 1970s, whereas the monsoon climate has become arid (Wang Pengxiang, 2007, [40]). The strength of the westerly wind index is a significant factor influencing the intensity of the westerly wind. For nearly 50 years, the westerly wind index in northwest China has demonstrated obvious cycle changes, with a trend of increasing strength over time, while both the East Asian summer and winter winds have shown a weakening trend (Li Wanli et al., 2008, [41]). Winter wind intensity has an oscillation cycle of 30–40 years, which reached its low-value period after 1980, and its intensity continues to decrease (Zhang Cunjie et al., 2002, [42]). Meanwhile, since 1970, the summer wind index has undergone rapid changes, and its intensity has continued to decrease in recent years (Guo Qiyun et al., 2003, [43]). Furthermore, Arctic Oscillation (AO) has a considerable

influence on the dry and wet climate changes in the study area. The AO index is closely associated with dry–wet variations in northwest China, with strong AO index years leading to increased precipitation in the northwest and decreased precipitation in the east, while the AO index was significantly strengthened before and after 1987, leading to increased water vapor transport to the west of the study area and a significant humidity trend (Peng-Xiang Wang, 2007b, [44]).

In terms of the spatial pattern, the drought occurring in the study area showed an overall trend of moderation in the northwest and aggravation in the southeast, which is consistent with the result of other studies. In terms of the division of arid subregions, Li Liang et al. [45] also used the REOF method to analyze the annual SPEI values, dividing the whole of Gansu into four drought-sensitive regions: the eastern, northwestern, central, and southeastern regions. It was found that drought was exacerbated in the southeast and moderated in the central part of the Hexi Corridor. Liu Bingxin et al. [46] divided Gansu into six climatic regions and discovered a trend of aridification shown in two parts of the southeast throughout the time series (1961–2014). The above results are consistent with the finding that a trend of aggravation was shown in the Hedong region and a trend of moderation was shown in the Wushaoling region. Although the drought occurring in Hexi showed a general trend of moderation, it was significant only in summer, with variations shown between different seasons. Wushaoling showed a trend of moderated aridification from the interannual scale to the seasonal scale, reaching the most significant extent in winter. In addition, the meteorological drought occurring in this region is relatively sensitive to altitude, which makes it necessary to increase awareness via early warning of drought events in high-altitude regions. When the climate becomes significantly warm and humid in the central and western parts, their seasonal differences are also worthy of attention. The intensity of drought still shows an upward trend in spring across some regions, which has an important effect on dry farming in these regions. This is averse to the improvement of surface water conditions and the sustainable development of the natural environment. Longdong, the eastern part of the study area, is in the west of the Loess Plateau. As an integral part of the Loess Plateau, there is a large area of cultivated land, which makes it one of the regions with serious soil erosion in the middle and upper reaches of the Yellow River. Therefore, the significant increase in drought events during spring in recent years has not only disrupted agricultural production, but has also exacerbated the vulnerability of the local ecological environment, thus affecting the sustainable development of regional agriculture industries, ecological preservation and biodiversity.

## 5. Conclusions

- (1) This research reveals that the duration of drought in the study area increased by an average of 0.475 days per decade, with an initial extension followed by a contraction. The intensity of drought also increased, particularly after 2000, and there was a trend of drought reduction in the northwest and intensification in the southeast. Furthermore, the top five modes of REOF contributed 64.46% of the variance, and the study area was partitioned into five arid subregions: Hexi, eastern Hedong, central Hedong, Wushaoling and western Hedong.
- (2) On an interannual scale, meteorological drought in the Hexi region has significantly decreased since 1988 ( $p < 0.01$ ). Additionally, that in the central and eastern regions of Hedong gradually eased at the beginning of this century, while the Wuling region has seen a significant reduction in meteorological drought since 1975, forming a watershed between drought mitigation and intensified change in space. On a seasonal scale, summer drought in the Hexi region has eased in the Hexi region compared to spring and autumn. However, the spring and summer seasons of the western Hedong region saw an increase in drought intensity in 2002 and 2000, respectively. The central region of Hedong showed a trend of drought and the most severe spring drought, and the meteorological drought eased in all four seasons.

- (3) The meteorological drought in the study area is influenced by local climate and circulation factors, with the Hexi region and western region responding to precipitation changes in the central and eastern regions, and the Wushaling region responding to the variations in sunshine duration and altitude. NAO has a significant influence on summer drought in the study area, while ENSO has a major impact on spring and autumn droughts (particularly in spring). Additionally, AO has the most significant effects on winter drought in the study area.

**Author Contributions:** Conceptualization, Y.W. and F.D.; methodology, Y.W. and F.D.; writing—original draft preparation, Y.W.; writing—review and editing, Y.W., F.D., Y.C. and Y.Z.; supervision, F.D., Y.C. and Y.Z.; funding acquisition, Y.C. All authors have read and agreed to the published version of the manuscript.

**Funding:** This research is supported by the Open Research Fund of Key Laboratory of Engineering Geophysical Prospecting and Detection of Chinese Geophysical Society, CJ2021IC03.

**Conflicts of Interest:** The authors declare no conflict of interest.

## References

1. Wilhite, D.A. *Handbook of Weather, Climate, and Water: Atmospheric Chemistry, Hydrology, and Societal Impacts. Drought in the US Great Plains*; Wiley: Hoboken, NJ, USA, 2002; pp. 743–758.
2. Zhang, Q.; Zhang, L.; Cui, X.C.; Zeng, J. Progresses and Challenges in Drought Assessment and Monitoring. *Adv. Earth Sci.* **2011**, *26*, 763–778.
3. Sternberg, T. Regional drought has a global impact. *Nature* **2011**, *472*, 169. [[CrossRef](#)] [[PubMed](#)]
4. Grayson, M. Agriculture and drought. *Nature* **2013**, *501*, S1. [[CrossRef](#)]
5. Dai, A.G. Drought under global warming: A review. *Wiley Inter Discip. Rev. Clim. Chang.* **2011**, *2*, 45–65. [[CrossRef](#)]
6. Mu, W.; Yu, F.; Xie, Y.; Liu, J.; Li, C.; Zhao, N. The copula function-based probability characteristics analysis on seasonal drought & flood combination event on the North China Plain. *Atmosphere* **2014**, *5*, 847–869.
7. Tian, Y.N. Summary of national drought disasters in 2017. *Flood Drought Disaster* **2018**, *8*, 67–72. Available online: [https://kns.cnki.net/kcms2/article/abstract?v=3u0qIhG8C44YLTIOAiTRKibYIV5Vjs7i0-kJR0HYBJ80QN9L51zrP4Lhkt6n\\_JXdPUI2y296ltp4AcRySMu7Dnb8iVcYLbZ&uniplatform=NZKPT](https://kns.cnki.net/kcms2/article/abstract?v=3u0qIhG8C44YLTIOAiTRKibYIV5Vjs7i0-kJR0HYBJ80QN9L51zrP4Lhkt6n_JXdPUI2y296ltp4AcRySMu7Dnb8iVcYLbZ&uniplatform=NZKPT) (accessed on 25 May 2023).
8. Wang, J.S.; Guo, J.Y.; Zhou, Y.W.; Yang, L.F. Progress and Prospect on Drought Indices Research. *Arid Land Geogr.* **2007**, *30*, 61–67.
9. Bao, Y.X.; Meng, C.Y.; Shen, S.H.; Qiu, X.F.; Gao, P.; Liu, C. Temporal and Spatial Patterns of Droughts for Recent 50 Years in Jiangsu Based on Meteorological Drought Composite Index. *Acta Geogr. Sin.* **2011**, *66*, 599–608.
10. Cao, Y.Q.; Lu, L.; Zhang, L.X. Spatio-Temporal Characteristics of Meteorological Drought in Liaoning Province Based on Z Index. *Resour. Sci.* **2012**, *34*, 1518–1525.
11. Ren, Y.L.; Shi, Y.J.; Wang, J.S.; Li, Y.P.; Zhu, Y.J.; Yang, Z.H.; Wei, B.L. Spatial and temporal variation characteristics of drought in Northwest China during 1961–2009 with standardized precipitation index. *J. Glaciol. Geocryol.* **2013**, *35*, 938–948.
12. Vicente-Serrano, S.M.; Beguería, S.; López-Moreno, J.I. A multiscale drought index sensitive to global warming: The standardized precipitation evapotranspiration index. *J. Clim.* **2010**, *23*, 1696–1718. [[CrossRef](#)]
13. Zhang, Y.J.; Wang, C.Y.; Zhang, J.Q. Based on the SPEI index, the arid space-time distribution characteristics of the North China Winter Wheat Region are analyzed. *J. Ecol.* **2015**, *35*, 7097–7107.
14. Li, J.; Wang, Z.L.; Huang, Z.Q.; Zhong, R.; Zhuo, S.; Chen, X. Based on SPEI's southwest agricultural region meteorological drought time and space evolution characteristics. *Resour. Environ. Yangtze River Basin* **2016**, *25*, 1142–1149.
15. Xue, H.Z.; Li, Y.Y.; Dong, G.T. Analysis of Spatial-temporal Variation Characteristics of Meteorological Drought in the Hexi Corridor Based on SPEI Index. *Chin. J. Agrometeorol.* **2022**, *43*, 923–934.
16. Yang, R.; Geng, G.P.; Zhou, H.K.; Wang, T. Spatial-temporal evolution of meteorological drought in the Wei river basin based on, S.P.E.I.-P.M. *Chin. J. Agrometeorol.* **2021**, *42*, 962–974.
17. Shelton, S.; Ogou, F.K.; Pushpawela, B. Spatial-temporal variability of droughts during two cropping seasons in Sri Lanka and its possible mechanisms. *Asia-Pac. J. Atmos. Sci.* **2022**, *58*, 127–144. [[CrossRef](#)]
18. Liu, X.Y. Based on SPEI's analysis of the characteristics of time and space changes in China's century-old drought. *J. Water Constr. Eng.* **2018**, *16*, 228–232.
19. Li, M.; Wang, G.W.; Zhang, L.Z. Based on SPEI's arid zoning and its climate characteristics analysis in Northeast China. *Arid Zone Resour. Environ.* **2016**, *30*, 65–70.
20. Wang, D.; Zhang, B.; An, M.L. Based on SPEI Southwest nearly 53 a drought time-space feature analysis. *J. Nat. Resour.* **2014**, *29*, 1003–1015.
21. Lu, J.Y.; Yan, J.P.; Li, Y.J. Based on SPEI and the tour theory of Yungui region 1960–2014 drought time-time change characteristics. *Zhejiang Univ. J. Sci.* **2018**, *45*, 363–372.

22. Zhang, P.Y.; Wang, G.; Chen, Y.N. Based on the SPEI Index, the Central Asian region's drought time-space distribution characteristics. *Arid Zone Res.* **2020**, *37*, 331–340.
23. Qi, L.Q.; Su, X.L.; Feng, K. Multiscale Meteorological Drought in Northwest China Response to Circulation Factor, S. *Arid Zone Resour. Environ.* **2020**, *34*, 107–113.
24. Zhang, Q.; Yao, Y.B.; Li, Y.H.; Luo, Z.; Zhang, C.; Li, D.; Wang, R.; Wang, J.; Chen, T.; Xiao, G.; et al. Research progress and prospect on the monitoring and early warning and mitigation technology of meteorological drought disaster in northwest China. *Adv. Earth Sci.* **2015**, *30*, 196–213.
25. Fan, S.P. Variation tendency of potential evapotranspiration and aridity index in Central Gansu Province in recent 55 years. *J. Earth Environ.* **2018**, *9*, 173–181.
26. Wen, J.C.; Jing, Y.S.; Han, L.J. Simulation of Evapotranspiration for Paddy Rice in Low Hilly Red Soil Region Base. *Chin. J. Agrometeorol.* **2020**, *41*, 201–210.
27. Li, T.S.; Wang, S.; Zhuang, C.; Liu, T.G. Theory of travel and the application of the Copula function in the joint distribution of two-dimensional arid variables. *Arid Zone Resour. Environ.* **2016**, *30*, 77–82. Available online: <https://kns.cnki.net/kcms2/article/abstract?v=3uoqIhG8C44YLTIOAiTRKibYIV5Vjs7ijP0rjQD-AVm8oHBO0FTadrwVkHOqs169ILK0-HOzCz9PJ5-Arx2GpHlmwsHg0n6K&uniplatform=NZKPT> (accessed on 25 May 2023).
28. Norh, G.R.; Bell, T.L.; Cahalan, R.F.; Moeng, F.J. Sampling errors in the estimation of empirical orthogonal functions. *Mon. Weather Rev.* **1982**, *110*, 699–706. [[CrossRef](#)]
29. Den, D.W.; Allen, J.S. Rotary empirical orthogonal function analysis of currents near the Oregon Coast. *Am. Meteorol. Soc.* **1984**, *14*, 35–46.
30. Bernaola-Galván, P.; Ivanov, P.C.; Amaral, L.A.N.; Stanley, H.E. Scale invariance in the nonstationary of human heart rate. *Phys. Rev. Lett.* **2001**, *87*, 168105. [[CrossRef](#)]
31. Pei, Y.S.; Jiang, G.Q.; Zhai, J.Q. Theoretical framework of drought evolution driving mechanism and the key problems. *Adv. Water Sci.* **2013**, *24*, 449–456.
32. Ji, D.M.; Zhang, B.; Wang, D.; Ma, Q.; Zhang, Y.Z.; Zhao, Y.F.; Yousif, E.Y. Spatio-temporal Variation Characteristics of Spring and Summer Meteorological Drought and Its Relationship with Circulation Factors in Hedong Maize Planting Areas of Gansu Province. *J. Nat. Resour.* **2015**, *30*, 1547–1559.
33. Ji, D. *Application Analysis of Different Meteorological Drought Indicators in Gansu Province*; Northwest Normal University: Lanzhou, China, 2015.
34. Yu, S.Q.; Lin, X.C.; Xu, X.D. The climatic change in northwest China in recent 50 years. *Clim. Environ. Res.* **2003**, *8*, 9–18.
35. Wang, C.H.; Zhang, S.N.; Li, K.C.; Zhang, F.; Yang, K. Change characteristics of precipitation in northwest China from 1961 to 2018. *Chin. J. Atmos. Sci.* **2021**, *45*, 713–724.
36. Cao, Y.C.; Jiao, M.L.; Qin, T.; Guo, T. Variation characteristics and influencing factors of summer half-year precipitation in Hedong region of Gansu Province from 1973 to 2020. *Arid Land Geogr.* **2022**, *45*, 1695–1706.
37. Zhai, L.X.; Feng, Q. Dryness/wetness climate variation based on standardized precipitation index in northwest China. *J. Nat. Resour.* **2011**, *26*, 847–857.
38. Zhang, Y.Z.; Zhang, B.; Liu, Y.Y.; Zhang, D.; Wang, D.; Zhang, F.; Jia, Y. Is the Wushaoling the climate shift dividing line in Gansu Province? *J. Glaciol. Geocryol.* **2016**, *38*, 611–619.
39. Teng, S.C.; Zhang, M.; Teng, J.; Qiao, Q. Climatic change characteristics in Wushaoling region of Gansu Province during 1951–2016. *J. Arid Meteorol.* **2018**, *36*, 75–81+129.
40. Wang, P.X.; He, J.H.; Zheng, Y.F.; Zhang, Q. Aridity wetness characteristics over northwest China in recent 44 years. *J. Appl. Meteorol. Sci.* **2007**, *18*, 769–775.
41. Li, W.L.; Wang, K.L.; Fu, S.M.; Jiang, H. The interrelationship between regional westerly index and the water vapor budget in northwest China. *J. Glaciol. Geocryol.* **2008**, *30*, 28–34.
42. Zhang, C.J.; Xie, J.N.; Li, D.L.; Guo, H. Effect of East Asian monsoon on drought climate of northwest China. *Plateau Meteorol.* **2002**, *21*, 193–198.
43. Guo, Q.Y.; Cai, J.N.; Shao, X.M.; Sha, W. Interdecadal variability of East-Asian summer monsoon and its impact on the climate of China. *Acta Geogr. Sin.* **2003**, *58*, 569–576.
44. Wang, P.X.; He, J.H.; Zheng, Y.F.; Qiang, Z. Inter-decadal relationships between summer arctic oscillation and aridity wetness feature in northwest China. *J. Desert Res.* **2007**, *27*, 883–889.
45. Li, L.; Pich, L.; Cai, H.J. Analysis of drought time and space characteristics in Gansu Province based on standardized precipitation evapotranspiration index. *Agric. Res. Arid Areas* **2019**, *37*, 256–266.
46. Liu, B.X.; Wang, X.X.; Che, Y.C. Analysis of drought time and space changes in different climate regions in Gansu Province based on the SPEI Index. *J. Gansu Technol.* **2019**, *35*, 53–57.

**Disclaimer/Publisher's Note:** The statements, opinions and data contained in all publications are solely those of the individual author(s) and contributor(s) and not of MDPI and/or the editor(s). MDPI and/or the editor(s) disclaim responsibility for any injury to people or property resulting from any ideas, methods, instructions or products referred to in the content.